A study of the role of dislocation density, indium composition on the radiative efficiency in InGaN/GaN polar and nonpolar light-emitting diodes using drift-diffusion coupled with a Monte Carlo method

I-Lin Lu,[1] Yuh-Renn Wu,[1,a)] and Jasprit Singh[2]
[1]*Institute of Photonics and Optoelectronics and Department of Electrical Engineering, National Taiwan University, Taipei 10617, Taiwan*
[2]*Department of Electrical Engineering and Computer Science, University of Michigan, Ann Arbor, Michigan 48109, USA*

(Received 29 August 2010; accepted 3 November 2010; published online 28 December 2010)

In this paper, we apply the Poisson, drift-diffusion, and Schrodinger solver coupled with the Monte Carlo method to study the in-plane carrier dynamics in the InGaN c-plane and nonpolar plane quantum well light-emitting diode device. Carrier diffusion, scattering, radiative recombination, and trapping by dislocation defects in the quantum well are studied. The impact of carrier dynamics on the internal quantum efficiency (IQE) in the quantum well with different indium compositions, dislocation densities, polarization effect, and interface roughness is studied. Our results show that (for dislocations densities in typical devices) due to the large radiative lifetime from the quantum confined Stark effect, nonradiative recombination caused by the dislocation defects plays a dominated role in limiting the IQE. In the nonpolar quantum well, the IQE is much better than in the c-plane case but is still strongly influenced by dislocation density. Our results show that to achieve 100% IQE, the dislocation density levels need to be lower than 10^6 cm^{-2} and 10^7 cm^{-2} for c-plane and nonpolar plane InGaN quantum well, respectively. Our results are also compared with published experimental work and have shown a good agreement. © *2010 American Institute of Physics*. [doi:10.1063/1.3524544]

I. INTRODUCTION

In recent years, nitride based light-emitting diodes (LEDs) are playing a dominant role in solid state lighting.[1–5] It is known that at high power the device efficiency suffers efficiency droop. The efficiency droop[6–9] in InGaN/GaN quantum well LEDs has been investigated for a while but a clear reason for the droop problem has not yet been provided.[9–11] It is interesting that in spite of a high dislocation density ($>10^8$ cm^{-2}), the radiative efficiency is not low, especially at low current injection with low indium composition. The high performance of the blue or near UV LED suggests that dislocations may not be of importance in the LED performance. In most papers discussing the nonradiative effects, the nonradiative lifetime due to dislocation or defects is assumed to be given by $\tau_{nr}=100-10$ ns for analyzing the internal quantum efficiency (IQE). One may ask the question: Is the non-radiative lifetime independent of indium compositions? Once in the quantum well how do carriers reach the dislocations and defects?

Dai *et al.*[5] have shown through their experiments that nonradiative lifetime and IQE are strongly dependent on the injection carrier density and dislocation spacing in certain cases. Hence, it is important to make a more complete study on the lateral transport of free carriers once they are in the InGaN quantum wells. This transport occurring under very low electric field is important as it determines how carriers diffuse toward regions of dislocations or defects before they recombine radiatively. In order to study this phenomenon, we use the Monte Carlo approach.[12] The process allows us to include interface roughness scattering,[13] electron-electron scattering,[14,15] phonon scattering,[16] and charged dislocation scattering[17,18] while studying the lateral mobility and diffusion length of carriers in the InGaN quantum wells. We show that the lateral diffusion length strongly depends on the interface roughness, indium composition, and radiative lifetime. We will show that for the low indium composition, the dislocation plays a minimal role due to smaller quantum confined Stark effect (QCSE). However, for the higher indium composition, the dislocation density plays a dominant role in limiting IQE. The influence of junction temperature, quantum well width, defect trapping center size, and nonpolar structures have also been studied.

II. METHOD

We examine the LED problem in two related steps. The vertical transport in which carriers enter the quantum wells and the lateral transport within the wells which allow the carriers to sense the defects. The vertical transport involves carrier injection, band bending and is examined through the use of Poisson, Schrodinger, and drift-diffusion methods. To determine the lateral carrier transport in the InGaN quantum well LED, we apply the Monte Carlo method. Carriers in the active region, i.e., in the quantum well are quantized in the vertical direction and the injection carrier density and the quantum well shape is dependent on the applied bias. We use the one-dimensional Poisson, Schrodinger, and drift-diffusion equations solver[19] to calculate the carrier quantum confined states, carrier density under bias, and the relation of

a)Electronic mail: yrwu@cc.ee.ntu.edu.tw.

current density to carrier density. The spontaneous recombination rates $R_{sp}(\hbar\omega)$ (Ref. 20) for carriers with different energy is obtained from Fermi-golden rule where:

$$R_{\text{spon}}(\hbar\omega) = \frac{e^2 n_r \hbar\omega}{m_0^2 \varepsilon_0 c^3 \hbar^2} \sum_{i,j} \int \frac{2}{(2\pi)^2} d^2\vec{k} |\hat{a}\cdot\vec{p}_{i,j}|^2 \times \frac{1}{\sigma\sqrt{2\pi}} \exp\left[\frac{-(E_{i,j}-\hbar\omega)^2}{2\sigma^2}\right] f^e[E_i^e(\vec{k})] \times f^h[E_j^h(\vec{k})] (\text{cm}^{-2}\,\text{eV}^{-1}\,\text{s}^{-1}), \quad (1)$$

In the Monte Carlo method, due to the quantized effect in the quantum well, we need to use the two-dimensional (2D) scattering formalism in the Monte Carlo method. we include 2D scattering mechanisms such as the 2D polar optical phonon scattering, acoustic phonon scattering,[16] interface roughness scattering,[13] alloy scattering,[13] charged dislocation scattering,[17,18] and electron-electron scattering[14,15] to determine the carrier mobility, diffusion, trapping, and recombination processes. The detail 2D scattering formalisms can be found in Refs. 13–18. When the injection density is high, subband states are filled with carriers and final states for scattering are lowered. Therefore, the Fermi-Dirac distribution function is used to determine if the final scattering state is occupied or not and if the recombination process will be activated or not. After obtaining the lateral carrier mobility (we focus on electrons since the mobility of electron is much higher than holes to the lower effective mass) we calculate the lateral diffusion coefficient using Einstein relation and then obtain the diffusion length using the following:

$$D = \mu \frac{k_B}{T}, \quad (2)$$

$$l_D = \sqrt{D\tau_r}, \quad (3)$$

where D is the diffusion coefficient and l_D is the diffusion length. The radiative lifetime τ_r can be by obtained by

$$\tau_r = \frac{n_{2d}}{\int R_{sp}(\hbar\omega) d\hbar\omega}, \quad (4)$$

In our model the carriers diffuse laterally till they either recombine radiatively or encounter a defect. In a real device the defects are random in space and we simulate this by using a Monte Carlo process to place dislocation defects randomly in the quantum well with different average spacing (dependent on the dislocation density) as shown in Fig. 1. In the simulation process, the electron will diffuse randomly in the quantum well for a calculated radiative lifetime. During the diffusion process, if an electron enters within a cross section of the location of the dislocation defect, it will be captured by the dislocation defect and recombine nonradiatively. Otherwise, it will diffuse till it recombines radiatively. In both of these two conditions, the carriers lost are recorded for the statistical output. Finally, the IQE can be determined by

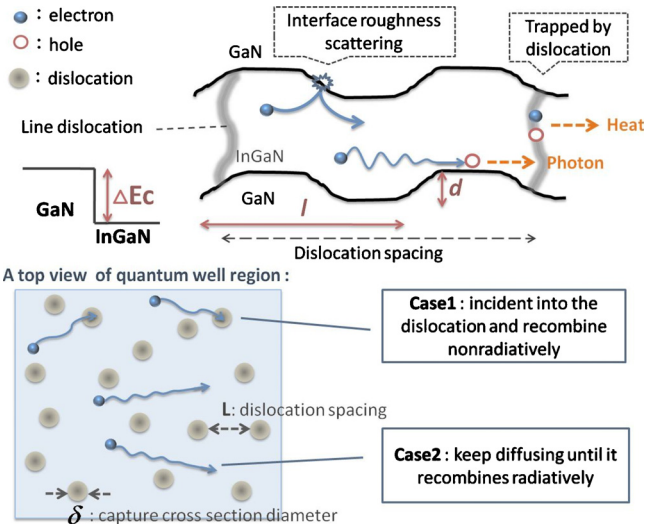

FIG. 1. (Color online) A Schematic of the interface roughness scattering, radiative, and nonradiative recombination mechanisms. The diagram also shows the definition of the scattering potential ΔE_c in the InGaN quantum well.

$$\eta_{IQE} = \frac{N_{rad}}{N_{rad} + N_{nonrad}}, \quad (5)$$

where N_{rad} is total counted number of radiative recombination and N_{nonrad} is total counted number of nonradiative recombination. Figure 1 also presents the definition of interface roughness length l, width d, and conduction band discontinuity potential, ΔE_c. The size of interface roughness and potential fluctuation ΔE_c also influence the carrier mobility significantly and limit the diffusion ability. The quantum well width W is assumed to be 3 nm in most cases. Hence, if the d is close to W, the structure has a very large interface roughness and the material may be thought of having indium clustering.

III. RESULTS

Figure 2 shows the calculated current versus average n_{2d} with different indium compositions in the six pair multiple quantum wells using our Poisson, drift-diffusion, and Schrodinger solver. The well width is 3 nm. We find the carriers will spill over the quantum well when the overall average n_{2d} in each quantum well is larger than $7-9\times10^{12}$ cm^{-2}. Also,

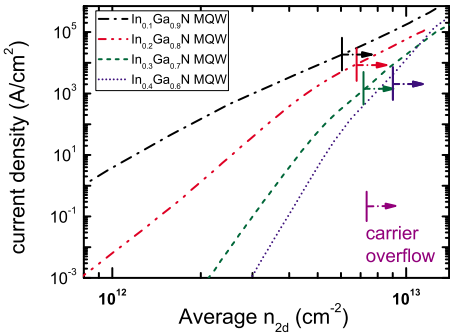

FIG. 2. (Color online) The calculated current density vs the average n_{2d} in the six pairs multiple quantum well with different indium compositions. We observed current overflow in the marked region.

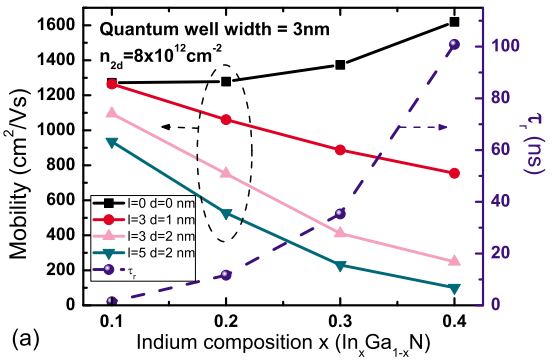

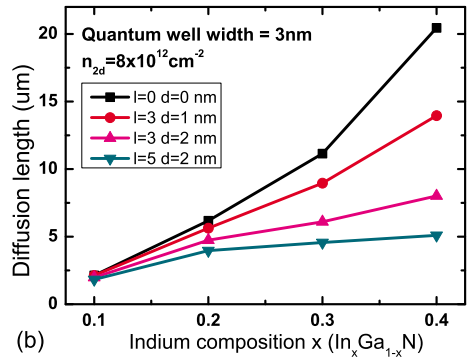

FIG. 3. (Color online) (a) The calculated mobility and radiative lifetime τ_r vs the indium composition with different interface roughness. The quantum well width is 3 nm and n_{2d} is 8×10^{12} cm^{-2}. (b) The estimated diffusion length vs the indium composition with different interface roughness.

the Auger effect might happen when the average n_{2d} is at this range. We find that the efficiency reaches the maximum when n_{2d} is near 8×10^{12} cm^{-2} since the influence of QCSE is reduced to a minimum by carrier screening. Therefore, in the results that follow, we set use a maximum n_{2d} equal to 8×10^{12} cm^{-2} to study the device characteristics.

To understand the carrier diffusion ability in the quantum well, we remove the defect traps in the beginning to obtain the carrier mobility and diffusion length. Figure 3(a) shows the calculated mobility and radiative lifetime versus indium composition when n_{2d} is equal to 8×10^{12} cm^{-2}. When the interface is perfect without surface roughness, the mobility of the higher indium composition is larger because of the smaller effective mass. The alloy scattering prevents the mobility from increasing too much as the effective mass decreases. If the interface is not perfect, the mobility drops rapidly with larger interface roughness especially for higher indium alloys. As shown in Fig. 3, the mobility decreases 20%–80% with larger interface roughness depending on the In composition. For example, when the carrier density is equal to 8×10^{12} cm^{-2} and $l=3$ nm, the mobility drops 12% for 10% indium content but drops 62% for 40% indium content if d increases from 1 to 2 nm. In addition, the strong piezoelectric field will push the carrier toward the interface so the interface roughness becomes more important. Note that as In content increases, the interface roughness scattering potential ΔE_c is larger.

Figure 3(b) shows the calculated lateral diffusion length. We can find that for the 10% indium composition, which is in the typical UV and blue LED range, the diffusion length is close to 1 μm because of the smaller QCSE and the smaller radiative lifetime. Therefore, for this composition it is possible to have a good IQE if the dislocation density is below 10^8 cm^{-2}. This also explains why the IQE is much better in the blue LED. However, as the indium composition increases up to more than 20%, which is in the typical green and yellow emission range, we can find that the radiative lifetime decreases significantly due to QCSE. Therefore, the overall diffusion length is larger than 2 μm, and the nonradiative process will dominate the system if the dislocation density is too large. For example, for the 40% indium case, the diffusion length is up to 10 μm without any interface roughness. Therefore, for this composition dislocation density has to be smaller than 10^6 cm^{-2} to minimize the influence of the nonradiative process. In addition, we can find that if the interface is very rough, i.e., as if there is indium clustering in the structure, the diffusion length and the nonradiative recombination rate decrease. This partially explains why the device can emit light with much higher indium composition and higher dislocation density. However, the IQE will be very low.

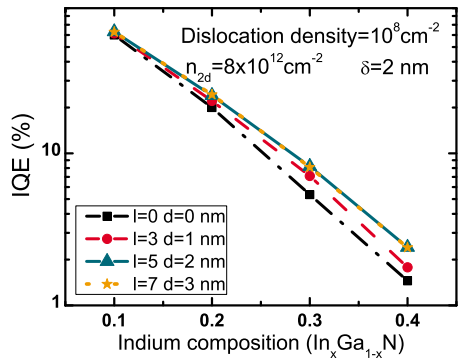

FIG. 4. (Color online) Estimated maximum efficiency vs indium composition for different roughness size values. The injected carrier density n_{2d} is 8×10^{12} cm^{-2}. The capture cross section diameter, δ is 2 nm.

A. The influence of the indium composition, interface roughness to the IQE

To discuss the IQE, we need to add the nonradiative recombination mechanism in the Monte Carlo program. As we mentioned earlier, the larger diffusion length will lead to a higher carrier capture rate. According to the results shown in Fig. 3(b), the higher In composition should have lower radiative efficiency due to the larger diffusion length. Figure 4 shows the estimated maximum efficiency versus the indium composition with different roughness when the dislocation density is 10^8 cm^{-2}. For the 10^8 cm^{-2} dislocation density, an average 1 μm dislocation spacing is distributed randomly in the quantum well as shown in Fig. 1. The dislocation spacing is randomly distributed in the quantum well with an assumed 1 μm average distance and the carrier capture cross section, δ, is assumed to be 2 nm in the Monte Carlo simulation. We found the IQE decreases rapidly as the indium composition increases because of the higher carrier capture rate. As shown, with a larger interface roughness, the IQE can be improved by a few percent to 40% (larger indium case) since the diffusion length is smaller as discussed above.

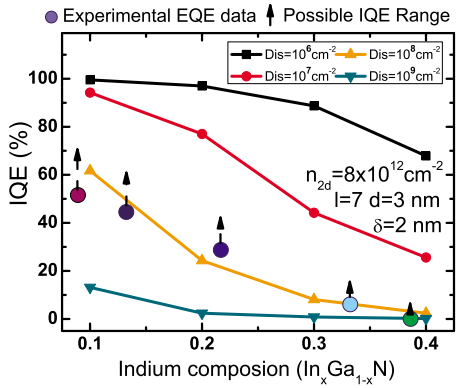

FIG. 5. (Color online) Estimated maximum efficiency vs indium composition for different dislocation density values when n_{2d} is 8×10^{12} cm^{-2}. Also shown is a comparison with experimental results (Ref. 21). The circles are the experimental results of EQE and the range bar is the estimated possible IQE range with an assumption of 70% light extraction efficiency.

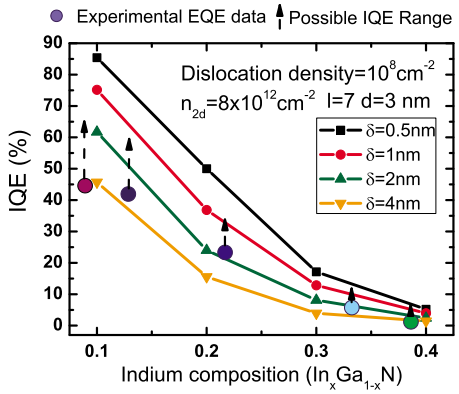

FIG. 6. (Color online) Estimated maximum efficiency vs indium composition for different capture cross section diameters when n_{2d} is 8×10^{12} cm^{-2}. The circle point is the experimental EQE result extracted from Ref. 21 and the range bar is the estimated possible IQE.

B. The influence of the dislocation density

We can expect that the higher dislocation density will lead to a higher capture rate. In Sec. III A, the diffusion lengths we have calculated are around 5–10 μm in most cases. This implies that to enhance the IQE, we need to have a lower dislocation or defect density. Figure 5 shows the estimated IQE versus the indium composition with different dislocation densities. If the device fabrication quality is improved and the dislocation density or defect density drops to 10^6 cm^{-2}, the IQE can be improved significantly. For example, the IQE can increase to 90% for 30% In composition and increase to 70% for 40% In composition if the dislocation or defect density is 10^6 cm^{-2}. For high performance green or yellow LEDs, it is necessary to reduce the dislocation density to be below 10^5 cm^{-2}. The circle points in Fig. 5 are the extracted external quantum efficiency (EQE) from experimental results.[21] The range bar is the estimated possible IQE range with an assumption of 70% light extraction efficiency. For a typical dislocation density 10^8 cm^{-2}, our results show a good agreement if an average 2 nm capture cross section is assumed. For the higher indium composition, the lattice mismatch is larger and it is harder to get a good crystal film even if the substrate is dislocation free. Therefore, it has been suggested that one use a thick InGaN buffer layer[22] to reduce the lattice mismatch in the system. This could be a possible solution to enhance the device performance.

C. The influence of the defect capture cross section

The carrier capture cross section size will affect the carrier capture directly. Published TEM results[23,24] show that the threading dislocation has a carrier trapping diameter of around a few nanometer. In our simulation, we change the capture cross section diameter within this range and try to estimate the expected IQE. The simulation results are shown in Fig. 6. Dislocation density of 10^8 cm^{-2} is assumed and the interface roughness $l=7$ nm, $d=3$ nm are applied. From the TEM result, the cross section in different locations is not a constant value. We try a range from 0.5 to 4 nm. Over this range, if the n_{2d} is 8×10^{12} cm^{-2}, we find that the efficiency for the 10% indium quantum well will change from 85% to 45%. Also, for the 40% indium, the efficiency of the LED will decrease from 5% to 1%. To obtain a better fitting, we compare to the experimental result[21] to get a better estimation. Our fitting shows that if the dislocation densities in the experimental results are around 10^8 cm^{-2}, we find that $\delta=2$ nm provides the best fit. We note that the dislocation density in the experimental results for different wavelength devices is not the same and the fitted δ may not present the exact case for the device. However, the value of δ is in a reasonable range and should be able to explain the trend in the experiments.

D. The influence of quantum well width and junction temperature

To study the influence of quantum well width on the LED performance, we assumed different well width (3, 4, and 5 nm) in the Poisson, Schrödinger, and drift-diffusion solver to obtain the carrier information and then calculated the mobility and diffusion length. The simulation results are shown in Fig. 7(a). We fixed the carrier concentration n_{3d} equal to 1.3×10^{19} cm^{-3} in each case and the dislocation density is 10^8 cm^{-2}. For the wider quantum width, the hole wave functions and electron wave functions are separated more, and the R_{sp} becomes smaller as the electron-hole overlap decreases. Although the carrier screening makes the overlap larger, band bending is still larger for wider quantum well and the radiative lifetime is much longer. Therefore, the efficiency becomes lower with larger quantum well width as shown in Fig. 7(a). It is to be noted that use of wider quantum well widths to increase the total amount of carriers in the quantum well is one way to reduce the carrier overflow and the Auger recombination. However, this also alters the nonradiative process and makes them more dominated.

Nonradiative recombination process will release energy leading to the heating of the junction. Unless the IQE becomes 100%, the device will heat up due to the energy loss. Figures 7(b) shows the IQE versus temperature with different values of the interface roughness. When the device is heated up to 400 K, the IQE drops around 30% to 40% because of the increase in τ_r. Therefore, the heating effect will make the

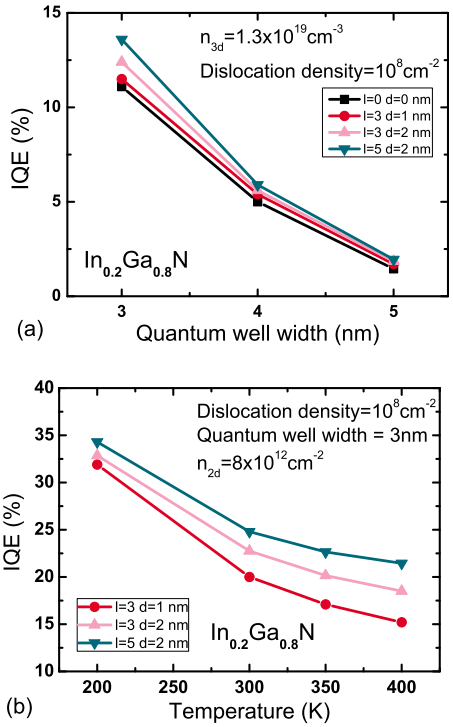

FIG. 7. (Color online) (a) Estimated maximum efficiency vs quantum well width with interface roughness. The value of n_{2d} is fixed at 1.3×10^{19} cm^{-3}. (b) Estimated maximum efficiency vs temperature with interface roughness when the n_{2d} is 8×10^{12} cm^{-2}. In both cases, the dislocation density is 1×10^{8} cm^{-2}, and δ=2 nm.

nonradiative process even more dominant and may lead to or worsen the droop effect at higher current density. It may appear that pulse measurement can completely remove the heating effect. However, the local heating effect at the active layer may not be avoided. In our previous studies we have studied the transient heating in the GaN heterojunction field effect transistor (HFET) devices[25] and found that the heat up time of the device in the active layer is only a few nanoseconds so that a very short pulse is needed.

E. Nonpolar structures

To achieve a better IQE it has been suggested to reduce the radiative lifetime by using the nonpolar[26,27] or semipolar[28,29] structures. Therefore, to investigate the influence of the nonpolar structure where there is no QCSE, we assumed the polarization charge difference at the heterointerface are zero in our Poisson, Schrödinger, and drift-diffusion solver and calculated the radiative lifetime (Table I). We then use the Monte Carlo method to estimate the radiative efficiency. Figure 8(a) shows the estimated IQE of nonpolar and c-plane InGaN quantum wells versus the indium composition when the dislocation densities are 10^7, 10^8, and 10^9 cm^{-2}. The red (solid) lines are for nonpolar structure and the black (dashed) lines are for c-plane structure. As we expected, the radiative lifetime becomes much smaller due to the larger spontaneous emission rate (R_{sp}). As shown in Fig. 8(a), the efficiency decreases rapidly with the indium composition in the c-plane structure due to the QCSE but IQE decreases only slightly with indium composition in the nonpolar structure. The reason for the slight decrease in

TABLE I. The material parameters (Ref. 30) for $In_xGa_{1-x}N$ at 300 K used in Poisson, Schrödinger, and drift-diffusion solver.

x	0.1	0.2	0.3	0.4
Bandgap (eV)	3.13	2.864	2.594	2.324
ε (ϵ_0)	10.713	11.146	11.579	12.12
ΔP (cm^{-2})	8.9×10^{12}	1.85×10^{13}	2.86×10^{13}	3.94×10^{13}
ΔE_c (eV)	0.179	0.361	0.544	0.727
$m_e^{\parallel}$ (m_0)	0.154	0.125	0.105	0.091
$m_e^{\perp}$ (m_0)	0.182	0.167	0.154	0.143
m_{hh} (m_0)	1.420	1.441	1.462	1.484

the nonpolar case with higher indium is due to the smaller effective mass and the larger mobility, which leads to the decrease in IQE as the indium composition increases. Therefore, the carrier diffuses much faster in the higher indium composition in the nonpolar case. However, even with nonpolar structure, we still find the efficiency would not be 100% if the dislocation density is high. It does improve a lot in the long wave range compared to the c-plane one but low dislocation and defect density conditions are still needed. Thus improvements in growth technology are needed to suppress defects beyond the current values.

If we assume the dislocation density to be 3×10^8 cm^{-2}, our simulation results show a good agreement with the experimental results[21] in low indium compositions as shown in Fig. 8(b). At higher indium composition, the experimental result shows lower IQE than we expect from

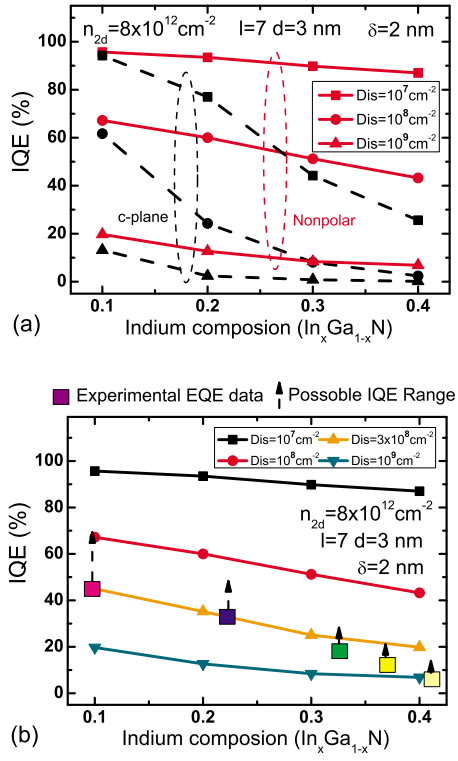

FIG. 8. (Color online) (a) Estimated efficiency vs indium composition when the dislocation densities are 10^7, 10^8, and 10^9 cm^{-2}. The solid lines are for a nonpolar structure and the dashed lines are for a c-plane structure. (b) Estimated efficiency vs indium composition with different dislocation densities. Also presented is a comparison with the experimental EQE results (Ref. 21) and the range bar is the estimated possible IQE range with an assumption 70% light extraction efficiency. Here δ is assumed to be 2 nm.

our simulations. We think that this is due to the difficulty of growing high quality samples at high In composition. If we want to fabricate yellow or green LEDs with higher IQE, low dislocation density, and reduced QCSE by nonpolar growth are both necessary.

IV. CONCLUSION

In conclusion, we have analyzed lateral dynamics of free carriers in the InGaN/GaN quantum wells using Monte Carlo methods. This has allowed us to examine lateral mobility, diffusion, and IQE. Our calculation shows the diffusion length is much longer than the dislocation spacing in current devices where typical dislocation density values are about (10^8 cm^{-2}). As the indium composition in the well increases, the diffusion length increases. As a result, carriers are trapped by dislocation defects and subsequently recombine nonradiatively. The most important reason for this unfavorable phenomenon is the long radiative lifetime resulting from the strong QCSE. From the simulation results, the IQE of 10% indium quantum well is about 60% but for 40% indium is only few percent if the dislocation density is 10^8 cm^{-2}. Since the IQE is not 100% in most cases, it is necessary to include the thermal effect in the studies. Our calculation also shows that the higher temperature leads to the decrease in IQE due to longer radiative lifetime and shorter nonradiative lifetime. Thus the heating effect will further reduce the IQE and contribute to the droop effect. We also have discussed how factors such as dislocation density, trapping cross section diameter, quantum well width, and use of nonpolar structures influence the IQE. Our studies show that with the nonpolar structure, the IQE does improve significantly but it will still not reach the 100% value if the dislocation density is high. Even with a nonpolar structure, the dislocation density levels need to be below 10^7 cm^{-2} if the IQE is to reach 100%.

ACKNOWLEDGMENTS

We would like to thank the support by National Science Council in Taiwan under Grant Nos. 98-2221-E-002-037-MY2 and 99-2221-E-002-058-MY3 and partially from Department of Energy under Grant No. DEFC2607NT43229.

[1]S. Nakamura, M. Senoh, N. Iwasa, S. Nagahama, T. Yamada, and T. Mukai, Jpn. J. Appl. Phys. Part 2 **34**, L1332 (1995).
[2]Y. Narukawa, J. Narita, T. Sakamoto, K. Deguchi, T. Yamada, and T. Mukai, Jpn. J. Appl. Phys. Part 2 **45**, L1084 (2006).
[3]E. F. Schubert, *Light-Emitting-Diodes* (Cambridge University Press, Cambridge, 2007).
[4]P. T. Barletta, E. A. Berkman, B. F. Moody, N. A. El-Masry, A. M. Emara, M. J. Reed, and S. M. Bedair, Appl. Phys. Lett. **90**, 151109 (2007).
[5]Q. Dai, M. F. Schubert, M. H. Kim, J. K. Kim, E. F. Schubert, D. D. Koleske, M. H. Crawford, S. R. Lee, A. J. Fischer, G. Thaler and M. A. Banas, Appl. Phys. Lett. **94**, 111109 (2009).
[6]M.-H. Kim, M. F. Schubert, Q. Dai, J. K. Kim, E. F. Schubert, J. Piprek, and Y. Park, Appl. Phys. Lett. **91**, 183507 (2007).
[7]Y. L. Li, R. Huang, and Y. H. Lai, Appl. Phys. Lett. **91**, 181113 (2007).
[8]M. F. Schubert, J. Xu, J. K. Kim, E. F. Schubert, M. H. Kim, S. Yoon, S. M. Lee, C. Sone, T. Sakong, and Y. Park, Appl. Phys. Lett. **93**, 041102 (2008).
[9]J. Hader, J. V. Moloney, B. Pasenow, S. W. Koch, M. Sabathil, N. Linder, and S. Lutgen, Appl. Phys. Lett. **92**, 261103 (2008).
[10]K. J. Vampola, M. Iza, S. Keller, S. P. DenBaars, and S. Nakamura, Appl. Phys. Lett. **94**, 061116 (2009).
[11]S.-H. Han, D.-Y. Lee, S.-J. Lee, C.-Y. Cho, M.-K. Kwon, S. P. Lee, D. Y. Noh, D.-J. Kim, Y. C. Kim, and S.-J. Park, Appl. Phys. Lett. **94**, 231123 (2009).
[12]M. Farahmand, C. Garetto, E. Bellotti, K. F. Brennan, M. Goano, E. Ghillino, G. Ghione, J. D. Albrecht, and P. P. Ruden, IEEE Trans. Electron Devices **48**, 535 (2001).
[13]M. Singh and J. Singh, J. Appl. Phys. **94**, 2498 (2003).
[14]M. Moko and A. Mokova, Phys. Rev. B **44**, 10794 (1991).
[15]O. Bonno, J. L. Thobel, and F. Dessenne, J. Appl. Phys. **97**, 043702 (2005).
[16]K. Yokoyama and K. Hess, Phys. Rev. B **33**, 5595 (1986).
[17]D. Jena, A. C. Gossard, and U. K. Mishra, Appl. Phys. Lett. **76**, 1707 (2000).
[18]N. G. Weimann, L. F. Eastman, D. Doppalapudi, H. M. Ng, and T. D. Moustakas, J. Appl. Phys. **83**, 3656 (1998).
[19]Y. R. Wu, M. Singh, and J. Singh, J. Appl. Phys. **94**, 5826 (2003).
[20]Y.-R. Wu, C. Chiu, C.-Y. Chang, P. Yu, and H.-C. Kuo, IEEE J. Sel. Top. Quantum Electron. **15**, 1226 (2009).
[21]J. S. Speck, Conference on Lasers and Electro-Optics (CLEO) The International Quantum Electronics Conference (IQEC), 1–6 May, 2009, Baltimore, Maryland (Optical Society of America, Washington, DC, 2009).
[22]T. L. Song, S. J. Chua, E. A. Fitzgerald, P. Chen, and S. Tripathy, Appl. Phys. Lett. **83**, 1545 (2003).
[23]E. Gaubas, S. Jursenas, S. Miasojedovas, J. Vaitkus, and A. Zukauskas, J. Appl. Phys. **96**, 4326 (2004).
[24]U. Bangert, A. Gutierrez-Sosa, A. J. Harvey, C. J. Fall, and R. Jones, J. Appl. Phys. **93**, 2728 (2003).
[25]Y.-R. Wu and J. Singh, J. Appl. Phys. **101**, 113712 (2007).
[26]H.-H. Huang and Y.-R. Wu, J. Appl. Phys. **106**, 023106 (2009).
[27]S. Ghosh, P. Waltereit, O. Brandt, H. T. Grahn, and K. H. Ploog, Phys. Rev. B **65**, 075202 (2002).
[28]H.-H. Huang and Y.-R. Wu, J. Appl. Phys. **107**, 053112 (2010).
[29]H. Sato, A. Tyagi, H. Zhong, N. Fellows, R. B. Chung, M. Saito, K. Fujito, J. S. Speck, S. P. DenBaars, and S. Nakamura, Phys. Status Solidi (RRL) **1**, 162 (2007).
[30]M. D. McCluskey, C. G. Van de Walle, C. P. Master, L. T. Romano, and N. M. Johnson, Appl. Phys. Lett. **72**, 2725 (1998).